Chemically Tuned Thin Elastomer Slab

Article *in* Molecular Crystals and Liquid Crystals · September 2008

DOI: 10.1080/15421400802240094

3 authors:

Paola castro-Garay
Universidad Estatal de Sonora
21 PUBLICATIONS **64** CITATIONS
SEE PROFILE

Adrian Reyes
Universidad Nacional Autónoma de México
140 PUBLICATIONS **637** CITATIONS
SEE PROFILE

Ruben Ramos-Garcia
Instituto Nacional de Astrofísica, Óptica y Elect…
127 PUBLICATIONS **588** CITATIONS
SEE PROFILE

Mol. Cryst. Liq. Cryst., Vol. 488, pp. 31–41, 2008

ISSN: 1542-1406 print/1563-5287 online
DOI: 10.1080/15421400802240094

Taylor & Francis
Taylor & Francis Group

Chemically Tuned Thin Elastomer Slab

P. Castro-Garay[1,2], J. A. Reyes[2], and R. Ramos-García[1]
[1]Depto De Óptica, Instituto Nacional De Astrofísica, Óptica y Electrónica, Puebla, Pue., México
[2]Depto Física Química, Instituto De Fisica, Universidad Nacional Autónoma De México, México Df Mexico

We have considered a cholesteric elastomer slab whose thickness is smaller than fifteen helix periods, immersed in a racemic solvent. We have calculated the reflectance and transmittance of obliquely incident circularly polarized light due to a cholesteric elastomer slab. We have found that even for such a thin slab there appears a regime of circular Bragg diffraction for certain values of the nematic penetration depth. We have also shown that for certain conditions on the solvent, the elastomer slab behaves as a universal filter. We summarize our work and address our conclusions.

1. INTRODUCTION

The Bragg phenomenon is shown by a sample of a material whose electromagnetic constitutive properties are periodically nonhomogeneous in the thickness direction. Its signature is very high reflectance in a certain wavelength-regime, provided the slab is thick enough to have a sufficiently large number of periods. This phenomenon is profited to design dielectric mirrors in optics [1].

If the material is isotropic, no dependence of the Bragg phenomenon on the polarization state of a normally incident electromagnetic wave is evident. The material must be anisotropic for the Bragg phenomenon to discriminate between two mutually orthogonal polarization states [2].

Periodicity comes from structural chirality in cholesteric liquid crystals and cholesteric elastomer [3], which exemplify structurally chiral

R. R.-G. acknowledges support from CONACyT Grant #45950 and Merck Mexico for financial support.

Address correspondence to P. Castro-Garay, Depto De Óptica, Instituto Nacional De Astrofísica, Óptica y Electrónica, Apdo p. 51, Puebla, Pue. 72000, México. E-mail: caspaoga@hotmail.com

BACK TO CONTENTS

materials. Both kinds of materials are continuously nonhomogeneous in the thickness direction where they show a helicoidal variation of anisotropy. Because the periodicity arises from structural chirality, incident electromagnetic plane waves of left- and right-circular polarization (LCP and RCP) states are reflected and transmitted differently in the Bragg wavelength-regime, and the Bragg phenomenon is then called the *circular* Bragg phenomenon. Exhibition of this phenomenon by cholesteric liquid crystals and chiral elastomers films emphasizes their use as circular-polarization rejection filters in optics [2,4].

The aim of this work is to analyze the behavior of the optical spectra corresponding to an elastomer slab whose thickness is smaller than fifteen helix periods, immersed in a chemical solvent. In particular, we like to discern if under this conditions the slab is able to perform as a as circular-polarization rejection filter.

2. ELASTIC FORMULATION

A cholesteric elastomer has locally a nematic structure. Consequently, the director vector $\hat{n} = (\cos\phi(z), \sin\phi(z), 0)$ is at x–y plane and $\phi(z)$ is the angle between director vector and x axis. The director vector has a continuous rotation as function of z, which describes a periodic helical structure characterized by a pitch p (or equivalent by wave number $q_0 = 2\pi/p$) [5,6].

The nematic penetration depth in rubbery networks is $\xi = \sqrt{K_2/D_1}$, where K_2 is the twist elastic constant and D_1 is local anchoring of the director to the rubbery network. The robustness of chiral imprinting depends on the nematic penetration depth ξ, which can be controlled by varying the density of cross-links in the network (affecting D_1) [7].

The imprinting efficiency depends on the chiral order parameter $\alpha = \xi q_0$, a function of elastic constant K_2 and D_1. A spectacular property of imprinted network is their capacity to preferentially absorb and retain right or left molecules from a racemic solvent.

When there is not deformation of the network, the energy for an elastomer formed under a cholesteric solvent which is subsequently replaced with an achiral one is given by [8],

$$F = \frac{1}{2}\int \left[K_2 \left(\frac{d\phi}{dz}\right)^2 + D_1 \sin^2(\phi - q_0 z) \right] dz. \tag{1}$$

To remove the chiral solvent, the Frank free energy to twist of director vector,

$$F_f = \frac{1}{2} K (\hat{n} \cdot \nabla \times \hat{n})^2 \tag{2}$$

BACK TO CONTENTS

associated with the first term of the Eq. (1)-tend to unwind the cholesteric helix but it finds resistance to rotate in the anchoring of the rubbery network-associate with the second term of Eq. (1). D_1 is proportional to rubbery elasticity modulus and the rubbery elasticity modulus is related with cross-linked density [7]. The scale length or nematic penetration depth rubbery at which the two energy contributions are comparable is usually small $\xi \simeq 10^{-8}\,\mathrm{m}$ for a typical $K_2 \simeq 10^{-11}\,\mathrm{J/m}$, $D_1 \simeq \mu(r-1)^2/r$, where $r \sim 0.9$ is the anisotropy chain number or cross-linked number and $\mu \simeq 10^5\,\mathrm{J/m^3}$ is the elasticity rubber modulus. The pitch is 10^3 bigger than nematic penetration depth ξ, then

$$\xi \ll p = \frac{\pi}{q_0}. \tag{3}$$

There are two forms of modifying this expression one of them is by enlarging the nematic penetration depth which amounts to do a weaker gel or low anisotropy one, the other is by increasing the Frank free energy. The chiral impression will be lost if D_1 diminishes, i.e., so that the director vector anchoring to rubbery will be almost null. Similarly, if the wave number q_0 or twist elastic constant K_2 are bigger the chiral impression will be also lost. The impression efficiency is reached for values of chiral parameter order $\alpha_c = \xi q_o$ lower than $2/\pi$ [8].

Equation (1) can be expressed in terms of nematic penetration depth parameter as,

$$F = \frac{1}{2}\int \left[\frac{\alpha^2}{q_0^2}\left(\frac{d\phi}{dz}\right)^2 + \sin^2(\phi - q_0 z)\right] \tag{4}$$

The equilibrium configuration can be obtained by minimizing F with respect to the angle, then we have got the Euler-Lagrange equations,

$$\partial_\phi F - \partial_z\left(\frac{\partial F}{\partial_z \phi}\right) = 0, \tag{5}$$

which in this case turns out to be

$$\frac{\alpha^2}{q_0^2}\frac{d^2\phi}{dz^2} + \sin 2(q_0 z - \phi) = 0. \tag{6}$$

Notice that if $\alpha = 0$ the solution of Eq. (6) is $\phi(z) = q_0 z$ which corresponds to an ideal or undistorted cholesteric helix. The general solution of Eq. (6) which is given by

$$\phi(z) = q_0 z - Am(cz/\xi, 1/c^2) + \pi/2, \tag{7}$$

BACK TO CONTENTS

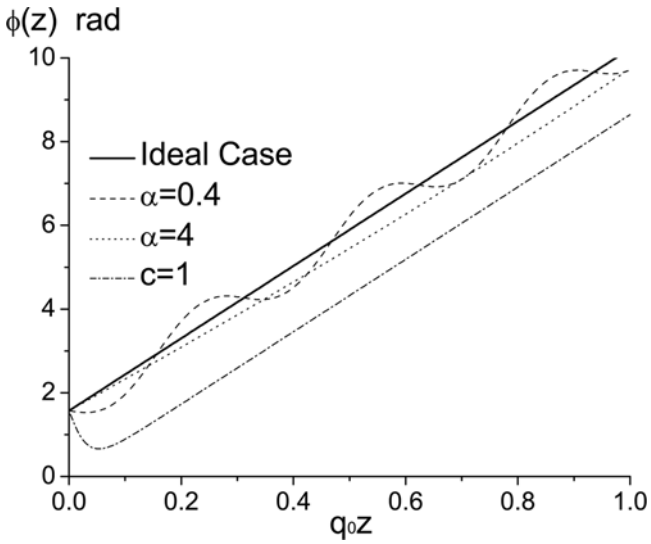

FIGURE 1 Director vector angle as function of position for different values of $\alpha = 0, 0.4, 4$ and $c = 1$.

where $Am(z,m)$ is the Jacobian amplitude and c is a constant related with the reduced elastic energy [8] $g = 2\xi F/TD_1$. The variation of c with the solvent is shown in Ref. [8]. In Figure 1 we show the director vector angle $\phi(z)$ against position for different values of chiral order parameter α and $c = 1$. It is interesting to note that by increasing α from zero, $\phi(z)$ presents oscillations without changing its amplitude, around the undistorted solution $\phi_0(z)$ whose spatial period increases, until reaches the critical values: $\alpha_c = 3$ and $c = 1$. After this value $\phi(z)$ deviate considerably from $\phi_0(z)$ and enlarges its effective q-value for $\alpha \geq \alpha_c$ which is equivalent to have an untwisted helix than that of $\phi_0(z)$.

3. OPTICAL DESCRIPTION

Let us consider an inhomogeneous material whose axis of chiral nonhomogeneity is along the z-axis, the optical relative permittivity matrix of the elastomer can be expressed

$$\bar{\epsilon}(z) = \begin{pmatrix} \epsilon_\perp + \epsilon_a \cos^2\phi & \epsilon_a \sin\phi\cos\phi & 0 \\ \epsilon_\perp \sin\phi\cos\phi & \epsilon_\perp + \epsilon_a \sin^2\phi & 0 \\ 0 & 0 & \epsilon_\perp \end{pmatrix} \tag{8}$$

BACK TO CONTENTS

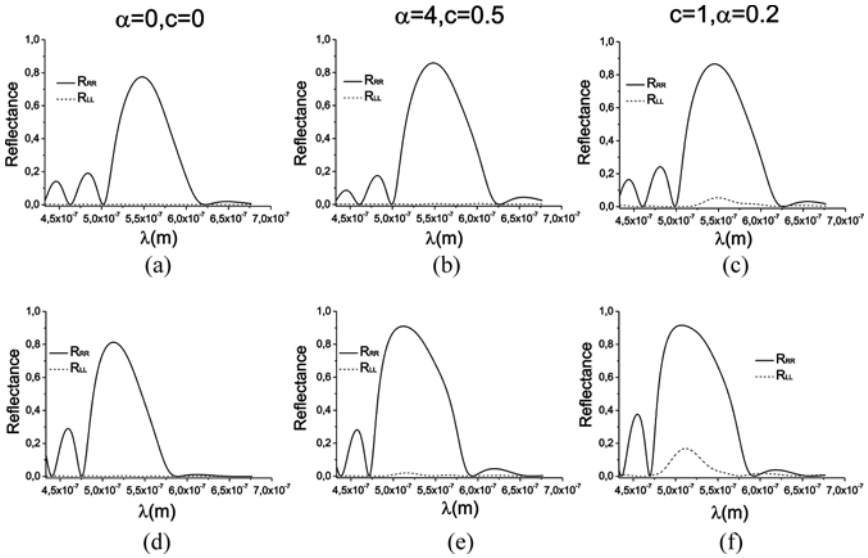

FIGURE 2 Circularly polarized reflectances R_{RR} and R_{LL} versus wavelength λ for a cholesteric elastomer slab of $10p$. In the absence of solvent ($\alpha = c = 0$) (a) $\theta = 45^\circ$ and (d) $\theta = 60^\circ$; for $\alpha = 4$, $c = 0.5$ with (b) $\theta = 45^\circ$ and (e) $\theta = 60^\circ$; and for $c = 1$, $\alpha = 0.2$ with (c) 45° and (f) 60°. Other parameters are $\epsilon_\perp = 1.91$, $\epsilon_\parallel = 2.22$, $h = 1$ and $p = 218\,\text{nm}$.

where $\epsilon_a = \epsilon_\parallel - \epsilon_\perp$ is the dielectric anisotropy with $\epsilon_\parallel$ and $\epsilon_\perp$ the dielectric constants in the optical regime parallel and perpendicular to the director $\hat{\mathbf{n}}$, respectively.

Maxwell equations for monochromatic fields of frequency ω in MKS units for a z-dependent medium, are given by

$$\left.\begin{aligned} \nabla \times \mathbf{E}(x,y,z) &= i\omega\mu_o \mathbf{H}(x,y,z) \\ \nabla \times \mathbf{H}(x,y,z) &= -i\omega\epsilon_o \bar{\epsilon}(z) \cdot \mathbf{E}(x,y,z) \end{aligned}\right\}, \quad 0 < z < L, \tag{9}$$

where ϵ_o and μ_o are the permittivity and the permeability of free space (i.e., vacuum). We shall assume a plane wave which impinges obliquely on the Cholesteric Elastomer. The z-components of Eq. (9) are algebraic equations that allow to express the z-components of the electric and magnetic fields E_z and H_z in terms of the transverse components E_x, E_y, H_x and H_y. Hence, to develope a complete description of the electromagnetic fields it is enough to follow a four-component vector formed with these

BACK TO CONTENTS

quantities, that is

$$\bar{\psi}(z) = \exp[i\kappa(x\cos\beta + ysin\beta)] \begin{pmatrix} e_x(z) \\ e_y(z) \\ h_x(z) \\ h_y(z) \end{pmatrix}, \tag{10}$$

where $\kappa = k\sin\theta$ is the transverse component of the wave vector, β and θ are the incidence angles. The first one defined by the wave vector and the x-axis in the x–y plane and the second one defined by the wave vector and the normal to the slab. Notice that in this expression we are explicitly taking a plane wave dependence for the transverse coordinates x and y.

Inserting Eq. (10) into Eq. (9), we find a set of four first order differential equations that can then be written in the following matrix form [9].

$$\frac{d}{dz}\bar{\psi}(z) = i\overline{A}(z)\cdot\bar{\psi}(z)\,, \quad 0 < z < L\,, \tag{11}$$

where the 4×4 matrix is given by

$$\overline{A}(z) = \begin{pmatrix} 0 & 0 & 0 & \omega\mu_o \\ 0 & 0 & -\omega\mu_o & 0 \\ -\omega\epsilon_o\frac{\epsilon_{13}(z)\epsilon_{32}(z)}{\epsilon_{33}(z)} + \omega\epsilon_o\epsilon_{12}(z) & \omega\epsilon_o\frac{(\epsilon_{31}(z))^2}{\epsilon_{33}(z)} - \omega\epsilon_o\epsilon_{22}(z) & 0 & 0 \\ \omega\epsilon_o\epsilon_{11}(z) - \omega\epsilon_o\frac{(\epsilon_{31}(z))^2}{\epsilon_{33}(z)} & -\omega\epsilon_o\epsilon_{23}(z) + \omega\epsilon_o\frac{\epsilon_{31}(z)\epsilon_{32}(z)}{\epsilon_{33}(z)} & 0 & 0 \end{pmatrix}$$

$$+ \begin{pmatrix} -\frac{\kappa\sin\beta\epsilon_{32}(z)}{\epsilon_{33}(z)} & \frac{\kappa\sin\beta\epsilon_{31}(z)}{\epsilon_{33}(z)} & -\frac{\kappa^2\sin\beta\cos\beta}{\omega\epsilon_o\epsilon_{33}(z)} & -\frac{\kappa^2\sin^2\beta}{\omega\epsilon_o\epsilon_{33}(z)} \\ \frac{\kappa\cos\beta\epsilon_{32}(z)}{\epsilon_{33}(z)} & -\frac{\kappa\cos\beta\epsilon_{31}(z)}{\epsilon_{33}(z)} & \frac{\kappa^2\cos^2\beta}{\omega\epsilon_o\epsilon_{33}(z)} & \frac{\kappa^2\sin\beta\cos\beta}{\omega\epsilon_o\epsilon_{33}(z)} \\ \frac{\kappa^2\sin\beta\cos\beta}{\omega\mu_o} & \frac{\kappa^2\sin^2\beta}{\omega\mu_o} & -\frac{\kappa\cos\beta\epsilon_{13}(z)}{\epsilon_{33}(z)} & -\frac{\kappa\sin\beta\epsilon_{13}(z)}{\epsilon_{33}(z)} \\ -\frac{\kappa^2\cos^2\beta}{\omega\mu_o} & -\frac{\kappa^2\sin\beta\cos\beta}{\omega\mu_o} & -\frac{\kappa\cos\beta\epsilon_{23}(z)}{\epsilon_{33}(z)} & -\frac{\kappa\sin\beta\epsilon_{23}(z)}{\epsilon_{33}(z)} \end{pmatrix}. \tag{12}$$

and $\epsilon_{ij}(z)$ with $(i,\ j = 1,2,3)$ are the elements of the dielectric tensor given by Eq. (8).

For undistorted cholesterics it is usual to use the Oseen transformation defined by

$$B(z) = \begin{pmatrix} \cos\phi & \sin\phi & 0 & 0 \\ -\sin\phi & \cos\phi & 0 & 0 \\ 0 & 0 & \cos\phi & \sin\phi \\ 0 & 0 & -\sin\phi & \cos\phi \end{pmatrix}, \tag{13}$$

BACK TO CONTENTS

which for the special case of normal incidence ($\kappa = 0$) turns $\overline{A}(z)$ out into a constant matrix so that Eq. (11) can be analytically solved [10]. Nonetheless, for the general case upon substitution of Eq. (8) into Eq. (12), this matrix can be written as

$$\begin{aligned}\overline{A}(z) = &\begin{pmatrix} 0 & 0 & 0 & \omega\mu_o \\ 0 & 0 & -\omega\mu_o & 0 \\ \omega\epsilon_o \sin\phi\cos\phi & -\omega\epsilon_o(\epsilon_\perp + \epsilon_a \cos^2\phi) & 0 & 0 \\ \omega\epsilon_o(\epsilon_\perp + \epsilon_a \sin^2\phi) & -\omega\epsilon_o \sin\phi\cos\phi & 0 & 0 \end{pmatrix} \\ &+ \frac{\kappa^2}{\omega\epsilon_o\epsilon_\perp} \begin{pmatrix} 0 & 0 & -\sin\beta\cos\beta & -\sin^2\beta \\ 0 & 0 & \cos^2\beta & \sin\beta\cos\beta \\ 0 & 0 & 0 & 0 \\ 0 & 0 & 0 & 0 \end{pmatrix} \\ &+ \frac{\kappa^2}{\omega\mu_o} \begin{pmatrix} 0 & 0 & 0 & 0 \\ 0 & 0 & 0 & 0 \\ \sin\beta\cos\beta & \sin^2 u & 0 & 0 \\ -\cos^2\beta & -\sin\beta\cos\beta & 0 & 0 \end{pmatrix},\end{aligned} \tag{14}$$

Equation (11) can be solved numerically by using a piecewise homogeneity approximation method.

4. REFLECTION AND TRANSMISSION

By virtue of linearity, the solution of the 4×4 mastrix ordinary differential Eq. (11) must be of the form

$$\bar{\psi}(z_2) = \overline{U}(z_2 - z_1) \cdot \bar{\psi}(z_1). \tag{15}$$

The procedure to obtain the unknown reflection and transmission amplitudes thus involves the 4×4 matrix relation

$$f_{exit} = \overline{U}(L) \cdot f_{entry}, \tag{16}$$

where the column 4-vectors

$$f_{entry} = \frac{1}{\sqrt{2}} \begin{pmatrix} (r_L + r_R) + (a_L + a_R) \\ i[-(r_L - r_R) + (a_L - a_R)] \\ -i[(r_L - r_R) + (a_L - a_R)]/\eta_o \\ -[(r_L + r_R) - (a_L + a_R)]/\eta_o \end{pmatrix} \tag{17}$$

BACK TO CONTENTS

and

$$f_{exit} = \frac{1}{\sqrt{2}} \begin{pmatrix} t_R + t_R \\ i(t_R - t_R) \\ -i(t_R - t_R)/\eta_o \\ (t_R + t_R)/\eta_o \end{pmatrix} \tag{18}$$

contain $\eta_o = \sqrt{\mu_o/\epsilon_o}$ as the intrinsic impedance of free space.

The reflection amplitudes $r_{L,R}$ and the transmission amplitudes $t_{L,R}$ can be computed for specified incident amplitudes (a_L and a_R) by solving (16). Interest usually lies in determining the reflection and transmission coefficients entering the 2×2 matrixes in the following two relations:

$$\begin{pmatrix} r_L \\ r_R \end{pmatrix} = \begin{pmatrix} r_{LL} & r_{LR} \\ r_{RL} & r_{RR} \end{pmatrix} \begin{pmatrix} a_L \\ a_R \end{pmatrix}, \tag{19}$$

$$\begin{pmatrix} t_R \\ t_R \end{pmatrix} = \begin{pmatrix} t_{LL} & t_{LR} \\ t_{RL} & t_{RR} \end{pmatrix} \begin{pmatrix} a_L \\ a_R \end{pmatrix}. \tag{20}$$

Both 2×2 matrixes are defined phenomenologically. The co-polarized transmission coefficients are denoted by t_{LL} and t_{RR}, and the cross-polarized ones by t_{LR} and t_{RL}; and similarly for the reflection coefficients in (20). Reflectances and transmittances aredenoted, e.g., as $T_{LR} = |t_{LR}|^2$.

5. RESULTS

We have calculated the co-polarized reflectance and transmittances of thin slabs of cholesteric elastomers of thickness 8, 10, and 15 spatial periods p. We have used the physical parameters of a real cholesteric elastomer materials [5,11]. In Figures 2–4 we compare R_{RR} and R_{LL} for thin elastomer slabs in the presence and absence of solvent. As the elastomer slab gets thinner the band reflection turns out to be less developed in the absence of the solvent as can be seen in most of these figures where amplitude reductions are obtained after diminish the thickness from 15 to 10 periods. Even larger reductions are observed for oblique incidence.

In Figures 2b and 2e we show R_{RR} and R_{LL} for obliquely incident light at $\theta = 45^\circ$ and 60°, which shines an elastomer slab whose thickness is $10\,p$ and which is distorted by a solvent that render the value $\alpha = 4$. Figures 2b and 2e show how the amplitude increases by 0.1 and the bandwidth enlarges by $\simeq 10\,\text{nm}$ with respect to the plots

BACK TO CONTENTS

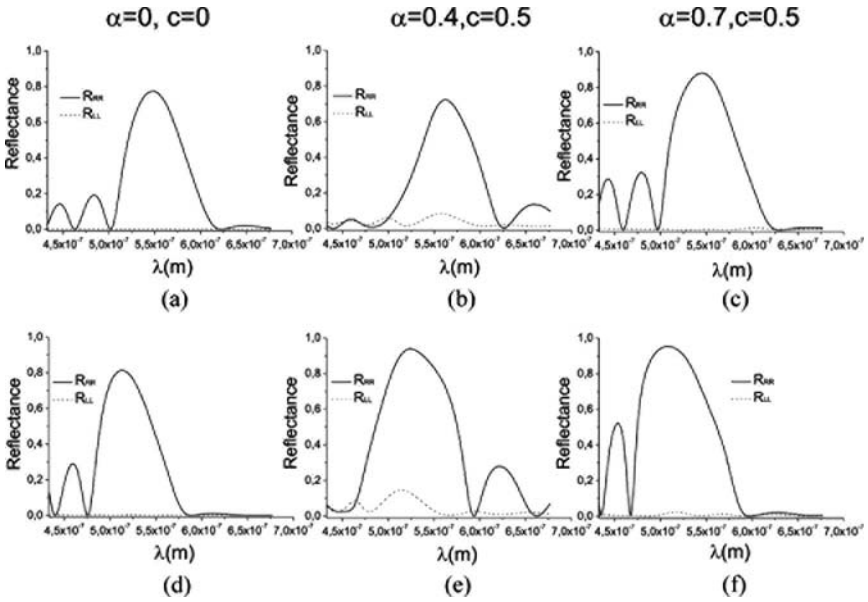

FIGURE 3 Circularly polarized reflectances R_{RR} and R_{LL} against λ for a cholesteric elastomer slab of $10p$. In the absence of solvent ($\alpha = c = 0$) (a) $\theta = 45°$ and (d) $\theta = 60°$; for $\alpha = 0.4$, $c = 0.5$ with (b) $\theta = 45°$ and (e) $\theta = 60°$; and for $\alpha = 0.7$, $c = 0.5$ with (c) $\theta = 45°$ and (f) $\theta = 60°$.

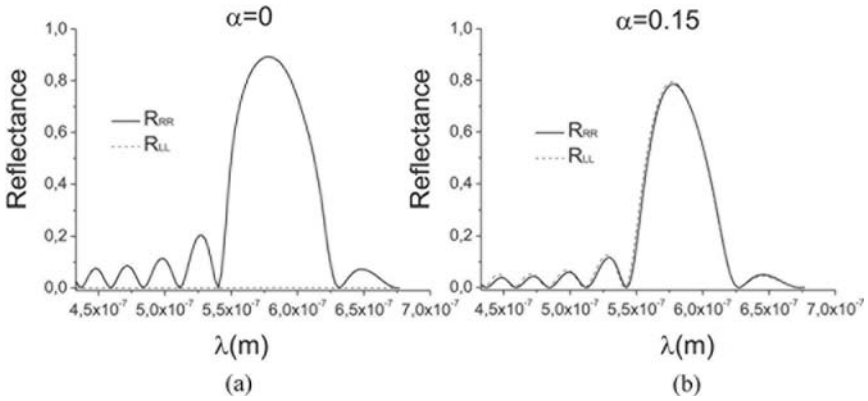

FIGURE 4 Circularly polarized reflectances R_{RR} and R_{LL} as function of λ for $\theta = 33°$, a slab thickness of $15p$. (a) In the absence of solvent ($\alpha = 0$) and (b) for $\alpha = 0.15$, $c = 0.5$.

BACK TO CONTENTS

corresponding to an undistorted material ($\alpha = 0,\ c = 0$) shown, respectively, in Figures 2a and 2d. On the other hand, R_{LL} almost do not exhibit any band reflection. The same changes for R_{RR} can be attained by setting $c = 1$ for oblique incidence at 45° and 60° but a very small amplitude reflection band is obtained for R_{LL}.

Figure 3 shows other examples of circularly polarized filters of $10\,p$ thickness whose band amplitude and bandwidth are enhanced chemically by a solvent. From these plots Figure 3b, represents an exception since for $\alpha = 0.4$ and $\theta = 45°$, R_{RR} diminishes in amplitude and bandwidth. In contrast, Figure 3e for $\theta = 60°$ and the same α, the band amplitude and bandwidth of R_{RR} enlarges by 15% and 20 nm, respectively. Also Figure 3c exhibits for $\theta = 45°$ and $\alpha = 0.7$ a R_{RR} reflection band corresponding to a distorted cholesteric elastomer whose amplitude and bandwidth has an augment of 10% and 10 nm in comparison with the undistorted case ($\alpha = 0$). The Figure 3f shows the same the Figure 3c, but for $\theta = 60°$, there is an increment of 15% in the R_{RR} reflection band amplitude and 20 nm in its bandwidth.

In Figure 4b for $\alpha = 0.15$ and thickness $15\,p$ we can observe a universal filter since both R_{RR} and R_{LL} exhibit the same band reflections for oblique incidence around 33°. For shorter thicknesses: 10 and 8 the band amplitudes decrease 20% and 40%, respectively. In fact, this also happens for some other proposed artificial structures [12] where the longitudinal modulation of the helix is not described by a function of the type given by Eq. (6), but instead by a harmonic function whose amplitude is larger than π.

Finally, we have not found reflection bands of any polarization when the light impinges elastomer slabs thinner than $8\,p$, whether the slab is immersed or not in a racemic solvent.

6. CONCLUSIONS

We have calculated the circularly polarized reflectances and transmittances as function of the chiral order parameter of a cholesteric elastomer immersed in a racemic solvent. The presence of the solvent on a thin slab ($15\,p$, $10\,p$ and $8\,p$) is able to increase the bandwidth and amplitude of the band reflection of R_{RR} by keeping R_{LL} without band, only for incidence angles $\theta \geq 45°$ and for $\alpha = 4$ and $c = 1$.

We have also exhibited that a $15\,p$, elastomer slab behaves of a universal filter, in the sense that presents band reflections for any polarization, for $\alpha = 0.15$ and $\theta = 33°$. This amount to have a chemically controlled filter which changes from the circularly Bragg phenomenon to a universal filter because of the presence of the solvent.

BACK TO CONTENTS

In summary, we have theoretically demonstrated that it is possible to construct very thin filters immersed in a racemic solvent that exhibit the circular Bragg phenomenon for oblique incidence.

REFERENCES

[1] Macleod, H. A. (2001). *Thin-Film Optical Filters*, 3rd ed., Institute of Physics Publishing: Bristol, United Kingdom.
[2] de Gennes, P. G. & Prost, J. (1993). *The Physics of Liquid Crystals*, Clarendon Press: Oxford, UK, (Chap. 6); Avendaño, C. G., *et al.* (2005). *J. Phys. A Math. Gen.*, *38*, 8821–8840.
[3] Warmer, M. & Terentjev, E. M. (2003). *Liquid Crystal Elastomers*, Oxford University Press: Chap 9; Mao, Y. & Warner, M. (2001). *Phys. Rev. Lett.*, *86*, 5309.
[4] Lakhtakia, A. & Messier, R. (2005). *Sculptured Thin Films: Nanoengineered Morphology and Optics*, SPIE Press: Bellingham, WA, USA (Chap. 9).
[5] Margarita, R. & Adrian, R. (2007). *J. Appl. Phys. Lett.*, *90*, 023513.
[6] Cicuta, P., Tajbakhsh A. R., & Terentjev, E. M. (2004). *Phys. Rev. E*, *70*, 011703.
[7] Courty, S., Tajbakhsh, A. R., & Terentjev, E. M. (2003). *Phys. Rev. Lett.*, *91*, 085503.
[8] Mao, Y. & Warner, M. (2000). *Phys. Rev. Lett.*, *84*, 5335.
[9] Marcuvitz, N. & Schwinger, J. (1951). *J. Appl. Phys.*, *22*, 806.
[10] Becchi, M., Ponti, S., Reyes, J. A., & Oldano, C. (2004). *Phys. Rev. B*, *70*, 033103.
[11] Cicuta, P., Tajbakhsh, A. R., & Terentjev, E. M. (2002). *Phys. Rev. E*, *65*, 051704.
[12] Sarkissian, H., *et al.* (2006). *Opt. Lett.*, *31*, 1678.

BACK TO CONTENTS